Turkish Journal of Electrical Engineering and Computer Sciences

Volume 26 | Number 4 Article 17

1-1-2018

Novel modified impedance-based methods for fault location in the presence of a fault current limiter

JAVAD BARATI

AREF DOROUDI

Turkish Journal of Electrical Engineering & Computer Sciences

http://journals.tubitak.gov.tr/elektrik/

Research Article

Turk J Elec Eng & Comp Sci
(2018) 26: 1881 – 1893

doi:10.3906/elk-1711-127

Novel modified impedance-based methods for fault location in the presence of a fault current limiter

Javad BARATI, Aref DOROUDI*
Department of Electrical Engineering, Shahed University of Technology, Tehran, Iran

Received: 14.11.2017 • **Accepted/Published Online:** 06.04.2018 • **Final Version:** 27.07.2018

Abstract: A fault current limiter (FCL) is promising novel electric equipment to effectively reduce excessive short circuit current in power networks. The presence of a FCL at the time of a fault occurrence makes it necessary to consider new settings for protective relays and fault locators. This paper examines the presence of a FCL in power networks and its effects on single-ended impedance-based fault location methods. It will be shown that FCL deployment in a transmission line makes the traditional fault location method inefficient. Two modified methods are presented to solve the problem. The modified methods locate the fault point using remote bus impedance in the presence of the FCL. The accuracy of the proposed methods is validated using the IEEE 14-bus system. The simulation results indicate that the proposed methods have considerable superiority over the conventional technique and perform well for different faults and FCL types.

Key words: Fault location, fault current limiter, single-ended impedance method

1. Introduction

Providing a continuous and reliable energy supply is the main objective of power systems. Nowadays, any power outage in a power grid creates heavy economic losses for industry and domestic consumers. Occurrence of random and unpredictable faults in power grids is a major cause of power outages. Accuracy in establishing the location of a fault accelerates line restoration and minimizes the losses due to power outages.

So far, several techniques have been proposed for fault location [1–3]. The analytical methods used for fault location reported in literature are divided into 3 general categories: impedance-based methods, traveling wave-based methods, and methods based on the high-frequency components of current and voltage. Traveling wave-based methods have a complex structure and need auxiliary equipment [4]. High-frequency components methods generally use wavelets or s-transforms. Implementation of these transforms is too expensive because of their relatively high-rate sampling filters [5–7]. Impedance-based methods, as the most common and practical methods, have a comparatively simple structure and can be easily implemented on digital protective relays. These methods employ fundamental components of voltage and current signals and they are divided into 2 categories: single-ended terminal and double-ended terminals approaches [8–11]. The single-ended approach employs just the data measured from the local (sending end) terminal of the protected line. The accuracy of the single-ended approach depends on the fault resistance value, fault type, and homogeneity of the transmission line [12]. The double-ended approach receives measured data from both local and remote (receiving end) terminals.

*Correspondence: doroudi@shahed.ac.ir

These methods are more accurate than single-ended methods because of their independence from fault resistance and fault type. However, the double-ended approach requires 2 datasets: time-synchronized measured data from both the sending and receiving end terminals [13].

Eriksson et al. suggested a highly accurate single-ended approach for fault location [14]. The method uses source impedances as known parameters to overcome any error caused by fault resistance, load current, or system nonhomogeneity. The Eriksson method also estimates the value of fault resistance. Indication of fault resistance aids in identifying the fault quickly and facilitates repair and restoration. In this method, the grid under consideration is first decomposed into 2 parts, prefault and pure-fault networks, by using the superposition theorem. The current distribution factor obtained from the prefault network is then applied to the pure-fault network to locate the fault point [14].

On the other hand, power system expansion and more interconnections in them, along with more dispersed generation (DG) deployment, have resulted in fault current amplitude increment. In some areas, the fault current amplitude has reached a level that may cause all the equipment to experience thermal and mechanical overstresses. Fault current limiters (FCLs) appear as innovative technical solutions, which can be deployed in power networks to limit the current under fault conditions [15,16]. They are generally divided into reactance and resistance types. FCLs only respond during the fault duration. In normal conditions, they do not act and appear as a nonimpedance element. A resistive FCL has a coil of superconductive material mounted in series in the line. In the case of a line fault, the coil that is initially in the superconducting state is driven to the normal state and the coil resistance appears on the line and limits the fault current. The inductive limiter, in its simplest form, consists of 2 windings connected in parallel. This combination is made so that the impedance of all is the lowest possible in normal conditions. During a fault, one of the coils (superconducting material) converts to its normal state and the other (copper) limits the current through the line.

The authors in [17] studied the application of a FCL in a power system and its effect on the simple reactance fault location method. The simple reactance method takes advantage of the fact that fault impedance is resistive in nature. The proposed method implies an iteration process to calculate the remote terminal impedance and subsequently fault current and location.

This paper assesses the fault location issue in the presence of FCLs by means of the Eriksson method. As will be shown, the conventional Eriksson method requires knowing the exact values of prefault currents. According to the absence and presence of a FCL in the normal and faulty conditions, the formal Eriksson method cannot exactly determine the fault location. In this paper, the Eriksson method is modified in such a way that fault location is possible in the presence of a FCL. This goal is achieved by using 2 different modified noniterative methods and estimation of grid currents before a fault beginning event.

The paper is organized as follows: in Section 2, the basic theory of the conventional Eriksson method for fault location is presented, while Section 3 demonstrates the modified Erikson methods. In Section 4, the accuracy of the proposed method is evaluated by simulation of the IEEE 14-bus network. Finally, Section 5 concludes the paper.

2. Theory of impedance-based fault location algorithms

Figure 1a shows a simplified grid under normal operating conditions without the FCL. The figure shows a generator and a transmission line, both connected in series to the external network. The external network is represented as a Thevenin model, i.e. a voltage source $\vec{E}_{Th}$ in series with impedance Z_{Th}. The exact and regular locations of measuring devices (CT and PT) are specified in Figures 1. The locations of the CT and

FCL are interchangeable because they are in series connection. However, the PT should measure the busbar voltage (busbar PT).

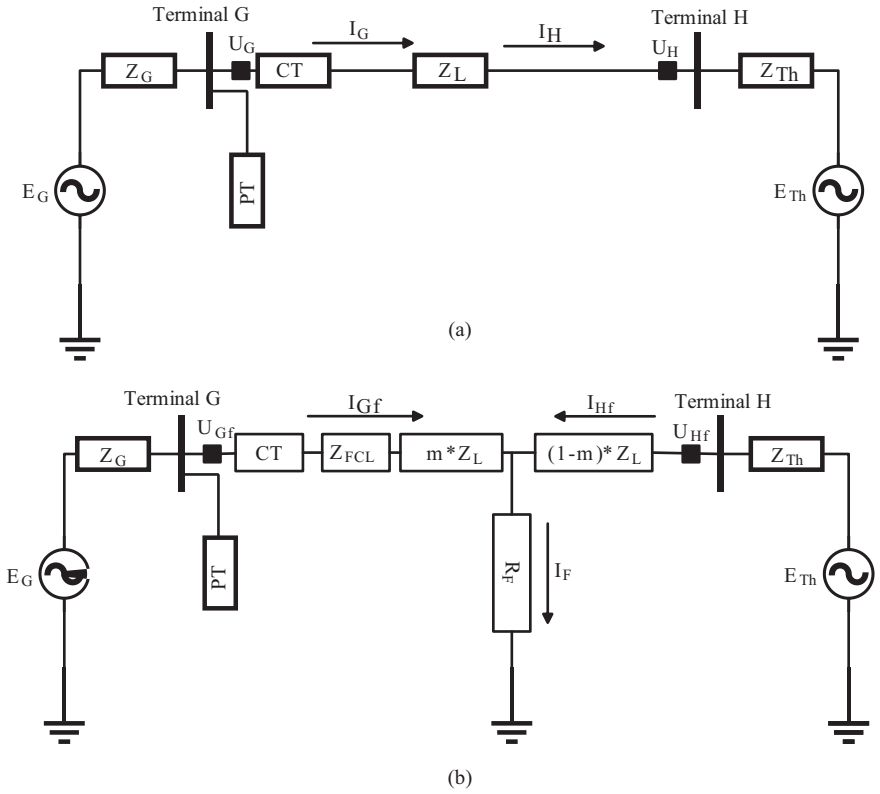

Figure 1. Fault on transmission line: (a) prefault system and (b) system during fault.

In the occurrence of a fault in the line, the FCL appears as an impedance to reduce the short circuit current (Figure 1b). Prefault and postfault voltages and currents can be measured by metering devices, which have been installed at terminal G. In this paper, the FCL is assumed to appear as a step input at the time of fault occurrence. In reality, the FCL appears exponentially by a time constant of about 1 ms [18]. This time constant is ignored throughout the rest of the paper since it has no noticeable effect upon the analysis.

As mentioned, single-ended methods only use measured data from one terminal (terminal G) and enjoy the advantage of not requiring a data link from the remote end. Because of dependency of the single-ended approach on the fault type (single line to ground (SLG), line to line (LL), double lines to ground (LLG) and 3-phase (LLL) faults), and in order to use identical parameters in the future calculations, the data of Table 1 are presented [12]. Based on these data, hereafter, notations $\vec{U}_{Gf}, \vec{I}_{Gf}$, and $\Delta\vec{I}_{Gf}$ are used for any fault type calculations, where $\vec{U}_{Gf}$ is the line-to-ground voltage during a fault, $\vec{I}_{Gf}$ is the line current during a fault, and $\Delta\vec{I}_{Gf}$ is the pure-fault current, all at terminal G. The related measures can be obtained from the table for any fault types.

According to Figure 1b and in the absence of the FCL, $\vec{U}_{Gf}$ can be expressed as [9,14]:

$$\vec{U}_{Gf} = m\, Z_L \vec{I}_{Gf} + R_F\, \vec{I}_F, \tag{1}$$

Table 1. Definition of U_{Gf}, I_{Gf}, and ΔI_{Gf} for different fault types.

Fault type	U_{Gf}	I_{Gf}	ΔI_{Gf}
A-G	U_{Gfa}	$I_{Gfa} + K * I_{Gf0}$	$I_{Gfa} - I_{Ga}$
B-G	U_{Gfb}	$I_{Gfb} + K * I_{Gf0}$	$I_{Gfb} - I_{Gb}$
C-G	U_{Gfc}	$I_{Gfc} + K * I_{Gf0}$	$I_{Gfc} - I_{Gc}$
AB, AB-G, ABC	$U_{Gfa} - U_{Gfb}$	$I_{Gfa} - I_{Gfb}$	$(I_{Gfa} - I_{Ga}) - (I_{Gfb} - I_{Gb})$
BC, BC-G, ABC	$U_{Gfb} - U_{Gfc}$	$I_{Gfb} - I_{Gfc}$	$(I_{Gfb} - I_{Gb}) - (I_{Gfc} - I_{Gc})$
CA, CA-G, ABC	$U_{Gfc} - U_{Gfa}$	$I_{Gfc} - I_{Gfa}$	$(I_{Gfc} - I_{Gc}) - (I_{Gfa} - I_{Ga})$
$K = (\frac{Z_{L0}}{Z_{L1}}) - 1$			

where m is the fraction of the total line length, Z_L is the line impedance, R_F is the fault resistance, and $\vec{I}_F$ is the fault current.

The apparent impedance measured from terminal G ($Zapp$) is given by:

$$Zapp = \frac{\vec{U}_{Gf}}{\vec{I}_{Gf}} = m\,Z_L + R_F \frac{\vec{I}_{Gf} + \vec{I}_{Hf}}{\vec{I}_{Gf}} = m\,Z_L + R_F \frac{\vec{I}_F}{\vec{I}_{Gf}}, \tag{2}$$

where $\vec{I}_{Hf}$ is the line current during a fault at terminal H. Eq. (2) is the base and main equation of the single-ended fault location method. In this equation, m, R_F, and $\vec{I}_F$ are unknown. In order to determine the fault location, R_F and $\vec{I}_F$ should be eliminated from this equation.

2.1. Eriksson method

The accuracy of single-ended methods heavily depends on fault resistance and inhomogeneity of transmission line. The Eriksson method uses both impedances behind sending and receiving ends of transmission line terminals (source impedances of side-G and side-H) to reduce this dependency [14]. Lack of information about these impedances may pose some problems for the Eriksson method. In the method, using the superposition principle, the faulted circuit is divided into 2 independent and individual circuits: prefault and pure-fault circuits (Figure 2). Indeed, to cover the load current effects, the actual voltages and currents can be considered to be composed of the prefault values plus the changes caused by the fault.

The fault point voltage ($\vec{U}_{f1pre}$) appears at the fault point under the prefault conditions and it is assumed as the driving voltage in a pure-fault network producing the changes caused by the fault event. Using the pure-fault network, the current distribution factor ($\vec{I}_F$ versus $\Delta\vec{I}_{Gf}$) can be calculated as follows:

$$\vec{I}_F = \left(\frac{Z_G + Z_L + Z_H}{(1-m)\,Z_L + Z_H}\right) \Delta\vec{I}_{Gf}, \tag{3}$$

where Z_G and Z_H are the source impedances of side-G and side-H.

Assuming the same current distribution factor in the prefault network and substituting Eq. (3) in Eq. (1), the following equation can be derived:

$$\vec{U}_{Gf} = m\,Z_L\,\vec{I}_{Gf} + R_F \left(\frac{Z_G + Z_L + Z_H}{(1-m)\,Z_L + Z_H}\right) \Delta\vec{I}_{Gf}. \tag{4}$$

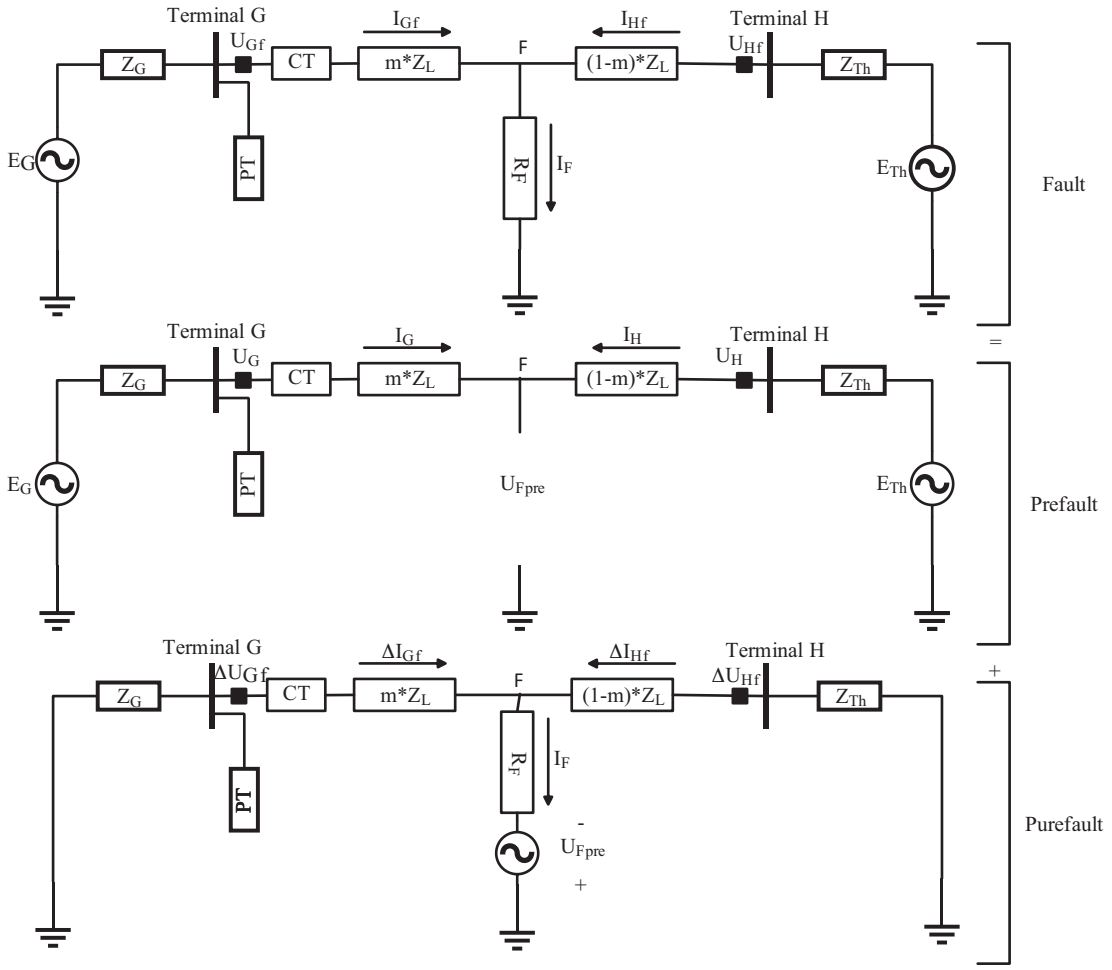

Figure 2. Superposition theorem used to decompose the faulted network.

After some manipulation, a quadratic equation can be obtained based on m and R_f:

$$m^2 - K_1 m + K_2 - K_3 R_F = 0, \tag{5}$$

$$\begin{aligned} K_1 &= a + j\,b = 1 + \tfrac{Z_H}{Z_L} + \left(\tfrac{\vec{U}_{Gf}}{Z_L \times \vec{I}_{Gf}}\right) \qquad K_2 = c + j\,d = \tfrac{\vec{U}_{Gf}}{Z_L \times \vec{I}_{Gf}} \left(1 + \tfrac{Z_H}{Z_L}\right) \\ K_3 &= e + j\,f = \tfrac{\Delta\vec{I}_{Gf}}{Z_L \times \vec{I}_{Gf}} \left(1 + \tfrac{Z_H + Z_G}{Z_L}\right) \end{aligned}. \tag{6}$$

Then we have the following:

$$(m^2 - am + c + eR_F) + j(-b\,m + d - e\,R_F) = 0. \tag{7}$$

The complex expression of Eq. (7) contains the unknown parameters m and R_F. However, Eq. (7) can be separated into 2 real and imaginary simultaneous equations, which both must be zero. Hence, we have:

$$m = \frac{\left(a - \frac{e\,b}{f}\right) \pm \sqrt{\left(a - \frac{e\,b}{f}\right)^2 - 4\left(c - \frac{e\,d}{f}\right)}}{2}, \tag{8}$$

$$R_F = \frac{d - m\,b}{f}. \tag{9}$$

Z_G can be calculated using the measured data from faulty and normal conditions:

$$Z_G = -\frac{\vec{U}_{Gf} - \vec{U}_G}{\vec{I}_{Gf} - \vec{I}_G}. \tag{10}$$

3. Modified Eriksson methods in the presence of FCL

The conventional Eriksson method gives wrong results in the presence of a FCL. Exact determination of the prefault currents has a strong influence on the Eriksson method's results. Due to the absence of the FCL in the prefault network, the currents recorded by the meters do not contain the limiter effect. These wrong currents in the Eriksson equations result in an erroneous solution. To solve the problem, the prefault currents in the virtual presence of the FCL should be estimated. For this purpose, the Thevenin equivalent circuit of the remote terminal (terminal H) is obtained by means of short-circuit capacity (SCC) of this terminal and the measured voltages and currents of the sending bus. Two modified methods are presented in the following text.

3.1. The first modified Eriksson method

In this approach, line current during a fault at terminal H ($\vec{I}_{Hf}$) and the remote Thevenin equivalent model (Z_{Th} and $\vec{E}_{Th}$) are estimated from the prefault measured data of the local bus and the SCC of the remote terminal. The proposed algorithm is as follows:

1. In normal conditions, the remote-end bus voltage ($\vec{U}_H$) should be calculated from Eq. (11):

$$\vec{U}_H = \vec{U}_G - Z_L \times \vec{I}_G(Normal\,conditions). \tag{11}$$

2. Knowing the SCC of the remote-end terminal, the remote-end Thevenin equivalent impedance (Z_{Th}) can be calculated by the following equation:

$$Z_{Th} = \frac{1}{SCC^*}, \tag{12}$$

where the asterisk represents the complex conjugate.

3. The remote Thevenin equivalent voltage ($\vec{E}_{Th}$) should then be determined as follows:

$$\vec{E}_{Th} = \vec{U}_G - Z_L \times \vec{I}_G(Normal\,conditions) - Z_{Th} \times \vec{I}_G(Normal\,conditions). \tag{13}$$

4. Assuming that E_{Th} is constant, the virtual prefault current in the presence of FCL ($\vec{I}_G(virtual)$) will then be calculated as:

$$\vec{I}_G(virtual) = \frac{\vec{U}_G - \vec{E}_{Th}}{Z_{FCL} + Z_L + Z_{Th}}, \tag{14}$$

where Z_{FCL} is the FCL impedance. $\vec{I}_G(virtual)$ should be employed in the equations instead of measured current.

5. The rest of the calculations are performed like in the Eriksson method except that the coefficients of the quadratic equation are given by:

$$\begin{aligned} K_1 &= a + j\,b = \tfrac{1}{Z_L}\left(-Z_{FCL}+Z_L + Z_H + \tfrac{\vec{U}_{Gf}}{\vec{I}_{Gf}}\right) \\ K_2 &= c + j\,d = \tfrac{1}{Z_L}\left(\tfrac{\vec{U}_{Gf}}{\vec{I}_{Gf}} - Z_{FCL} + \tfrac{\vec{U}_{Gf}\times Z_H - Z_H \times Z_{FCL}\times \vec{I}_{Gf}}{Z_L \times \vec{I}_{Gf}}\right) . \\ K_3 &= e + j\,f = \tfrac{\Delta\vec{I}_{Gf}}{Z_L\times\vec{I}_{Gf}}\left(1 + \tfrac{Z_H+Z_G+Z_{FCL}}{Z_L}\right) \end{aligned} \tag{15}$$

3.2. The second modified Eriksson method

The circuit compensation theorem is used in the second modified method [19]. According to Ohm's law, when current flows through any resistor, there will be a voltage drop across the resistor. This dropped voltage opposes the source voltage. Hence, voltage drop across a resistance in any network can be assumed as a voltage source acting opposite to the source voltage. The compensation theorem states that any resistance in a branch of a linear electrical network can be replaced by a voltage source that provides the same voltage as the voltage dropped in the resistance replaced. In other words, in a linear time-invariant network when the resistance (R) of an uncoupled branch carrying a current (I) is changed by ΔR, the currents in all the branches will change and can be obtained by assuming that an ideal voltage source $(\vec{U}_C)$ has been connected such that $\vec{U}_C = \vec{I}(R+\Delta R)$ in series with $(R+\Delta R)$ when all other sources within the network are replaced by their internal resistances. Based on this theorem, the second modified algorithm is described as follows:

a. The current $\vec{I}_G$ is considered as prefault current (measured at a local bus) in the absence of a FCL and in prefault conditions.

b. The remote terminal voltage and Z_{Th} are calculated by Eqs. (11) and (12), respectively.

c. Voltage drop across the FCL $(\vec{U}_{FCL})$ is calculated as follows:

$$\vec{U}_{FCL} = Z_{FCL} \times \vec{I}_G. \tag{16}$$

d. $\vec{U}_{FCL}$ is inserted into the network as an ideal voltage source and network equivalent voltage sources are turned off (shorted).The network current in this situation $(\vec{I}_{FCL})$ is then calculated as:

$$\vec{I}_{FCL} = \frac{\vec{U}_{FCL}}{Z_G + Z_{FCL} + Z_L + Z_{Th}}. \tag{17}$$

e. Finally, the prefault current in the presence of the FCL is expressed as follows:

$$\vec{I}_G(virtual) = \vec{I}_G - \vec{I}_{FCL}. \tag{18}$$

f. Calculations will continue similarly to the first modified method.

4. Simulation results

In this section, the modified IEEE 14-bus system (Figure 3) is used to evaluate the proposed methods. It is assumed that the line between bus 1 and 5 is out of work. Simulations are carried out with DIgSILENT software and [20] is used to obtain the IEEE 14-bus system data. Fault location is done at the transmission line between buses 1 and 2, which are considered as the local and remote-end terminals, respectively. The FCL is near bus 1. Short circuit calculations are carried out, and the SCC at bus 2 is computed as 1170 MVA with $X/R = 10.9$. The fault location error is calculated as follows:

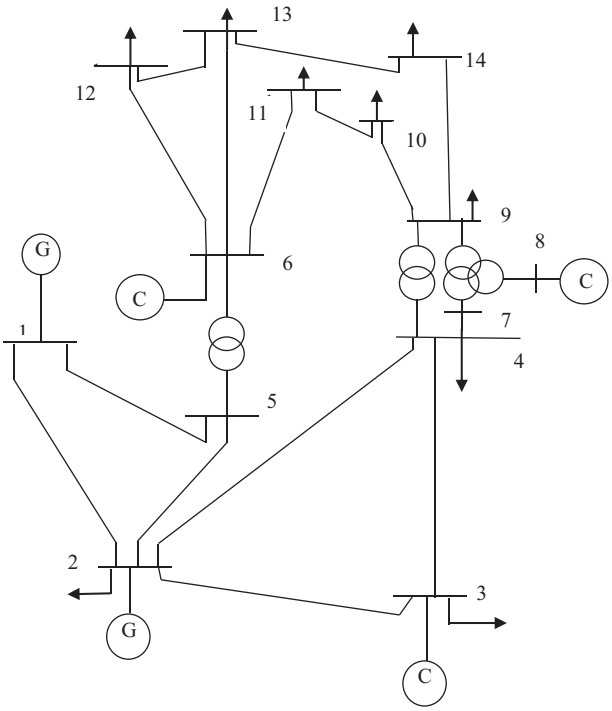

Figure 3. Single-line diagram of the IEEE 14-bus system.

$$\text{Error } (\%) = \frac{\text{Actual Location } - \text{ Estimated Location}}{\text{Total Line Length}} \times 100. \tag{19}$$

Three-phase faults are now simulated at various locations on the transmission line between bus 1 and bus 2. In impedance-based fault location methods, fundamental components of voltage and current are used for the calculations. It is noteworthy that DC offset and CT saturation may cause waveform distortion. In this case, some filters should be employed to accurately obtain the fundamental components of current and voltage signals. In this paper, the fast Fourier transform algorithm is used to estimate the fundamental components of voltage and current waveforms [21,22].

Table 2 shows the results of fault location using the conventional Eriksson method for various fault locations and for different values of fault resistance. The table depicts that in the presence of the FCL, the conventional Eriksson method cannot correctly estimate the fault location, especially at higher values of fault resistance. Incorrect estimation of prefault current is the major source of error. This is due to FCL's zero impedance appearance in normal conditions and before fault occurrence. To overcome the problem, estimating the prefault current in the virtual presence of the FCL is required.

Table 2. Estimated values by the conventional Eriksson method for LLL.

Exact location (pu)	Error (%)				
	$R_F = 2\ \Omega$	$R_F = 4\ \Omega$	$R_F = 6\ \Omega$	$R_F = 8\ \Omega$	$R_F = 10\ \Omega$
0.1	0.2	0.4	0.8	1.3	2.2
0.25	0.8	1.3	2	2.9	3.9
0.5	1.7	2.5	3.4	4.7	6.3
0.9	4.3	5.5	7.2	9.8	12.9

Table 3 shows the percentage error between the real and estimated values of fault locations obtained by the first modified method. As can be seen, the method estimates the fault locations more accurately than the conventional Eriksson method. However, approximate calculation of remote Thevenin voltage (Eq. (13)) is the major cause of inaccuracy. For more clarity, Figure 4 shows fault location percentage error versus different fault resistances for variations in fault location. The maximum error occurs at 90% of line length and with the fault resistance of 10Ω. As Figure 4 shows, with a constant fault resistance, the accuracy of the method reduces with the far-end faults. The reason is that fault current of the local terminal is known and measured, but the fault current from the remote end terminal is unknown and estimated. The higher the contribution of terminal H to the total fault current is, the less the accuracy of the fault location method will be. The figure also depicts that with a constant fault location, the accuracy of the method reduces as the fault resistance increases.

Table 3. Estimated values by the first modified Eriksson method for LLL.

Exact location (pu)	Error (%)				
	$R_F = 2\ \Omega$	$R_F = 4\ \Omega$	$R_F = 6\ \Omega$	$R_F = 8\ \Omega$	$R_F = 10\ \Omega$
0.1	0.2	0.4	0.8	1.3	2.2
0.25	0.8	1.3	2	2.9	3.9
0.5	1.7	2.5	3.4	4.7	6.3
0.9	4.3	5.5	7.2	9.8	12.9

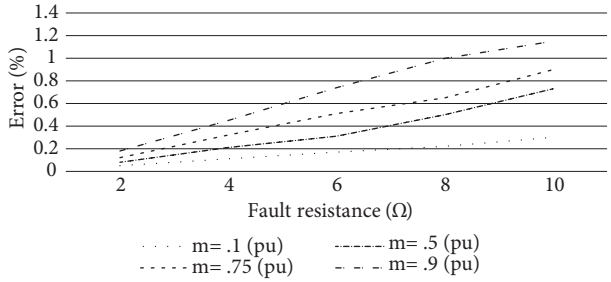

Figure 4. Percentage errors versus fault resistance and for different fault locations calculated by the first modified method, three-phase fault.

Table 4 shows the percentage error of fault location by the second modified method. As shown, the method presents good results for any fault resistances and locations. The accuracy of this method has greatly increased since the remote end voltage is not employed in the approach.

Table 4. Estimated values by the second modified method for LLL.

Exact location (pu)	Error percentage (%)				
	$R_F = 2\ \Omega$	$R_F = 4\Omega$	$R_F = 6\ \Omega$	$R_F = 8\ \Omega$	$R_F = 10\ \Omega$
0.1	0.02	0.8	0.15	0.2	0.27
0.25	0.03	0.1	0.18	0.29	0.4
0.5	0.05	0.17	0.29	0.48	0.63
0.9	0.14	0.36	0.63	0.9	1.02

To show the universality of the proposed methods, 2 different cases are also considered. The first case is a different fault type, i.e. a SLG fault. Tables 5 and 6 present the percentage error by the first and second proposed methods for a SLG fault for different fault locations and fault resistances. The algorithm is similar to the LLL case except that positive, negative, and zero sequence circuits should be applied to obtain the 3-phase voltages in Eq. (11):

Table 5. Estimated values by the first modified method for single-phase fault.

Exact location (pu)	Error percentage (%)				
	$R_F = 2!\Omega$	$R_F = 4\Omega$	$R_F = 6!\Omega$	$R_F = 8!\Omega$	$R_F = 10!\Omega$
0.1	0.08	0.16	0.28	0.36	0.46
0.25	0.1	0.2	0.34	0.5	0.68
0.5	0.13	0.29	0.44	0.6	0.82
0.9	0.25	0.56	0.86	0.95	1.32

Table 6. Estimated values by the second modified method for single-phase fault.

Exact location (pu)	Error percentage (%)				
	$R_F = 2\ \Omega$	$R_F = 4\Omega$	$R_F = 6\ \Omega$	$R_F = 8\ \Omega$	$R_F = 10\ \Omega$
0.1	0.06	0.14	0.24	0.33	0.42
0.25	0.08	0.13	0.3	0.45	0.61
0.5	0.11	0.2	0.38	0.54	0.74
0.9	0.23	0.46	0.74	0.88	1.18

$$\vec{U}_{Ha} = \vec{U}_{Ga} - [Z_{L0}\vec{I}_{G0} + Z_{L1}\left(\vec{I}_{G1} + \vec{I}_{G2}\right)], \tag{20}$$

$$\vec{U}_{Hb} = \vec{U}_{Gb} - [Z_{L0}\vec{I}_{G0} + Z_{L1}\left(a^2\vec{I}_{G1} + a\,\vec{I}_{G2}\right)], \tag{21}$$

$$\vec{U}_{Hc} = \vec{U}_{Gc} - [Z_{L0}\vec{I}_{G0} + Z_{L1}\left(a\,\vec{I}_{G1} + a^2\vec{I}_{G2}\right)]. \tag{22}$$

where $a = 1\angle -120$ and subscripts 1, 2, and 0 show positive, negative, and zero sequences of variables. The tables show that both of the proposed methods present high accuracy for SLG faults.

In the second case, instead of a resistive FCL, an inductive FCL is located on the transmission line. Table 7 shows the percentage error of fault location by the proposed methods for a LLL fault occurrence in the middle of the line and for $R_F = 4\Omega$. As can be seen in the table, the percentage errors for the inductive FCL are slightly more than that of the resistive FCL. However, they are still acceptable.

Table 7. Estimated values by the proposed methods: resistive and inductive FCLs.

$Z_{FCL}\ (\Omega)$	Error percentage (%)	
	First modified	Second modified
1.5	0.17	0.14
3	0.29	0.2
j1.5	1.25	1
j3	1.9	1.5

With the networks having multiple power corridors, fault location on a line will not be accurate if the influence of the remote-end in-feed duo to other transmission lines on the fault is not into account. In other words, one limitation of the Eriksson method is exclusion of the effect of multiple power corridors normally present in any power network. This drawback, when coupled with high resistance faults and faults nearer the receiving end, results in an erroneous solution. Several methods have been proposed to solve the problem [23–25]. The modified methods generally use the Thevenin theorem and provide a system or line model that is most suitable for representing the system conditions under a fault. A new current distribution factor is thus computed from the modified model. In this paper, we used the SCC of the remote-end bus to calculate the impedance of this terminal. The proposed methods are applied to a single-machine infinite-bus system. Modified methods, which have been proposed for inclusion of the effect of multiple power corridors, can be employed and adapted in our method too.

5. Conclusion

The presence of FCLs in power networks affects the accuracy of single-ended impedance-based fault location methods and may lead to the malfunction of the existing digital fault locator. The problem of the conventional method is the lack of prefault current in the presence of a FCL since the FCL appears only at the moment of fault occurrence. In this paper, 2 modified methods were presented to solve the problem. The proposed methods estimate the fault location in the presence of a FCL using the remote bus SCC. The accuracy of the proposed methods is verified using the IEEE 14-bus system. The maximum error occurs at 90% of line length and with fault resistance of 10Ω. For LLL (single-phase fault), the percentage errors are 1.15% (1.32%) and 1.02% (1.18%) for the first and the second modified methods, respectively. The simulation results indicate that the proposed methods have considerable superiority over the conventional method for different fault types and for resistive and inductive FCLs. The accuracy of the second modified method is higher than the first one as the remote-end voltage is not employed in this algorithm. Both methods can be easily implemented in existing digital protective relays.

Nomenclature

E_{Th}	Thevenin voltage at terminal H
U_{Gf}, U_{Hf}	Line-to-ground voltages during fault at terminals G and H
$\Delta U_{Gf}, \Delta U_{Hf}$	Pure-fault voltages during fault at terminals G and H
U_{Ga}, U_{Gb}, U_{Gc}	Prefault voltages in phases a, b, and c at terminal G
U_{Ha}, U_{Hb}, U_{Hc}	Prefault voltages in phases A, B, and C at terminal H
U_H	Prefault voltage at terminal H
I_{Gf}, I_{Hf}	Line currents during fault at terminals G and H
$\Delta I_{Gf}, \Delta I_{Hf}$	Pure-fault currents at terminals G and H
I_{Gf}, I_{Hf}	Current during fault at terminal G and H
Z_L	Line impedance between terminals G and H
Z_{FCL}	FCL impedance
Z_{Th}	Thevenin impedance at terminal H
Z_{L0}, Z_{L1}, Z_{L2}	Sequence components of the line impedance between terminals G and H
m	Per unit distance to the fault point
U_{G1}, U_{G2}, U_{G0}	Sequence components of the prefault voltages at terminal G
R_F $I_G(virtual)$	Fault resistance Prefault current in the virtual presence of FCL

References

[1] Jia H. An improved traveling-wave based fault location method with compensating the dispersion effect of traveling wave in wavelet domain. Math Probl Eng 2017; 6: 1-11.

[2] Koley E, Yadav A, Santosh Thoke A. A new single-ended artificial neural network-based protection scheme for shunt faults in six-phase transmission line. Int T Electr Energy 2015; 25: 1257-1280.

[3] Farshad M, Sadeh J. Generalized instance-based fault locating in transmission lines using single-ended voltage measurements. Int T Electr Energy 2015; 25: 799-816.

[4] Akmaz D, Mamiş MS, Arkan M, Tağluk ME Fault location determination for transmission lines with different series-compensation levels using transient frequencies. Turk J Elec Eng & Comp Sci 2017; 25: 3764-3775.

[5] Magnago FH, Abur A. Fault location using wavelets. IEEE T Power Deliver 1998; 13: 1475-1480.

[6] Kale V, Bedekar P. Fault location estimation based on wavelet analysis of traveling waves. In: Asia-Pacific Power and Energy Engineering Conference; 27–29 March 2012; Shanghai, China. New York, NY, USA: IEEE. pp. 27-29.

[7] Borghetti A. Continuous-wavelet transform for fault location in distribution power networks: definition of mother wavelets inferred from fault originated transients. IEEE T Power Syst 2008; 23: 380-388.

[8] Andrade De, Ponce T. Impedance-based fault location analysis for transmission lines. In: IEEE Transmission and Distribution Conference and Exposition; 7–10 May 2012; Orlando, FL, USA. New York, NY, USA: IEEE. pp. 1-6.

[9] Das S, Santoso S, Gaikwad A. Impedance-based fault location in transmission networks: theory and application. IEEE Access 2014; 2: 537-557.

[10] Liao Y. Fault location for single-circuit line based on bus impedance matrix utilizing voltage measurements. IEEE T Power Deliver 2008; 23: 609-617.

[11] Zhihan X, Zhang Z. What accuracy can we expect from the single-ended fault locator. In: 68th Annual Conference for Protective Relay Engineers; 30 March–2 April 2015; Collage Station, TX, USA. New York, NY, USA: IEEE. pp. 690-716.

[12] Ha HX, Zhang B, Lv ZL. A novel principle of single-ended fault location technique for EHV transmission lines. IEEE T Power Deliver 2003; 18: 1147-1151.

[13] Izykowski J. Accurate non-iterative fault-location algorithm utilizing two-end unsynchronized measurements. IEEE T Power Deliver 2011; 26: 547-555.

[14] Eriksson L, Saha MM, Rockefeller GD. An accurate fault locator with compensation for apparent reactance in the fault resistance resulting from remote-end in feed. IEEE T Power Ap Syst 1985; 104: 423-436.

[15] Park J, Seung-Ryul L, Yoon J. Application of bus-tie HTS-FCL on 154kV buses in the Korean power system. In: Transmission & Distribution Conference & Exposition: Asia and Pacific; 26–30 October 2009; Seoul, Korea. New York, NY, USA: IEEE. pp. 1-4.

[16] Chabanloo RM, Habashi EM. Farokhifar M. The effect of fault current limiter size and type on current limitation in the presence of distributed generation. Turk J Elec Eng & Comp Sci 2017; 25: 1021-1034.

[17] Barati J, Doroudi A. Fault location in transmission lines in the presence of fault current limiter. Journal of Iranian Association of Electrical and Electronics Engineers 2017; 14: 99-107 (article in Persian with an abstract in English).

[18] Sung BC, Park DK, Park JW. Study on a series resistive SFCL to improve power system transient stability: modeling, simulation, and experimental verification. IEEE T Ind Electron 2009; 56: 2412-2419.

[19] Bakshi UA, Bakshi AV. Electrical Circuit Analysis. 1st ed. Pune, India: Technical Publications Pune, 2008.

[20] Mishra P. Enhancement of voltage profile for IEEE-14 bus system by using STATIC-VAR compensation (SVC) when subjected to various changes in Load. International Journal of Research Studies in Science, Engineering and Technology 2014; 1: 27-33.

[21] Mamis MS, Arkan M. FFT based fault location algorithm for transmission lines. In: 7th International Conference on Electrical and Electronics Engineering; 1–4 December 2011; Bursa, Turkey. New York, NY, USA: IEEE. pp. 1-71.

[22] IEEE. Guide for Determining Fault Location on AC Transmission and Distribution Lines. IEEE Std. C37.114-2004. New York, NY, USA: IEEE, 2005.

[23] Saha MM, Wikstrom K, Izykowski J, Rosolowski E. New accurate fault location algorithm for parallel lines. In: Seventh International Conference on Developments in Power System Protection; 9–12 April 2001; Amsterdam, the Netherlands. New York, NY, USA: IEEE. pp. 407-410

[24] Naraendranath UA, Purushotham GK, Thukaram D, Parthasarathy K. Accurate fault location on EHV transmission line having parallel power corridors. In: 11th National Power System Conference; 2000; Bangalore, India. New York, NY, USA: IEEE. pp. 571-576.

[25] Lian B, Salama MM. A. An overview of the digital fault location algorithms for the power transmission line protection based on the steady-state phasor approaches. Electr Mach Pow Syst 1996; 24: 83-115.